

# Unique properties of plasma produced by Compact ECR Source in regions far away from resonance

A. Ganguli<sup>1</sup>, R. D. Tarey<sup>2</sup>, Ramesh Narayanan<sup>1</sup>

<sup>1</sup>Indian Institute of Technology, Centre for Energy Studies, Hauz Khas, New Delhi 110016, India

<sup>2</sup>Indian Institute of Technology, Department of Physics, Hauz Khas, New Delhi 110016, India

A novel Compact ECR Plasma Source (CEPS), developed at IIT Delhi, was used to produce plasma inside a test chamber. The magnet design and placement of the CEPS are such that the magnetic field in the test chamber is well below the resonance field, decaying exponentially along the axis with scale length  $\lambda_M \approx 9.2$  cm. The studies conducted in argon (0.5 – 10 mTorr) reveal that the plasma in the test chamber has two distinct electron populations, bulk ( $T_e \approx 2 - 3$  eV) and warm ( $T_w \approx 50 - 60$  eV), both of which are so strongly magnetized that their densities track the magnetic field profile accurately, decreasing exponentially with the scale length of the magnetic field ( $\approx \lambda_M$ ). The bulk electrons are in approximate thermal equilibrium, obeying the Boltzmann relation with a varying accuracy depending on the pressure. The plasma potential  $V_p$  varies linearly along the axis implying that the plasma is quasineutral. It can be shown that at relatively low pressures ( $\leq 0.5$  mTorr) the plasma in the test chamber is almost entirely due to outflow of plasma formed in the CEPS, while at high pressures ( $\geq 5$  mTorr) the plasma is formed by ionization by the warm electrons arriving from the CEPS even though their density is three orders lower.

## 1. Introduction

The compact electron cyclotron resonance (ECR) plasma source (CEPS) developed at IIT Delhi uses NdFeB ring magnets along with microwave launcher, impedance matching unit and mode converter integrated into it (gross length  $\approx 60$  cm, weight including magnets  $\approx 14$  kg) [1]. The magnet design ensures that the resonance zone is well localized within the plasma source section of the CEPS. In general, the flexibility and portability of the CEPS allows it to be used for producing plasma in systems of arbitrary shape and size. Recently, high density ( $\sim 10^{11}$  cm<sup>-3</sup>), uniform plasma have also been produced in a large volume ( $\sim$  few cubic meters), large diameter ( $\sim 1$  m) system by connecting several CEPS around the chamber periphery [2, 3].

To be able to use the CEPS effectively for a wide range of applications it is necessary to characterize the plasma produced by the CEPS in detail. The experimental results presented in this talk were obtained by connecting the CEPS to one end of a small test chamber of length  $\sim 37$  cm and diameter  $\sim 15$  cm (Fig. 1). The magnetic field of the CEPS expands into the chamber and plasma from the resonance region flows into the chamber. The plasma reveals some unique properties not usually seen in ECR produced plasmas.

A Langmuir probe (LP) inserted from a horizontal port opposite the CEPS port, was used for determining the bulk plasma density  $n_0$  and its

temperature  $T_e$ , the warm electron density  $n_w$  (if present) and its temperature  $T_w$ , and the plasma potential  $V_p$ . A National data acquisition card (NI 6143 S series) was used to control the LP power supply and collect the I-V data. The details of LP procedure, its utility and validity, and analysis of plasma parameters from the I-V data can be found from the reported literature [1-5].

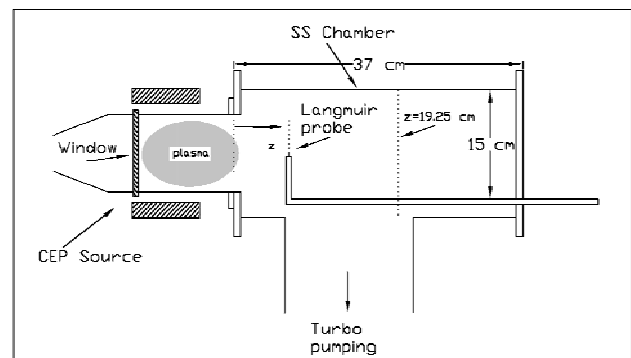
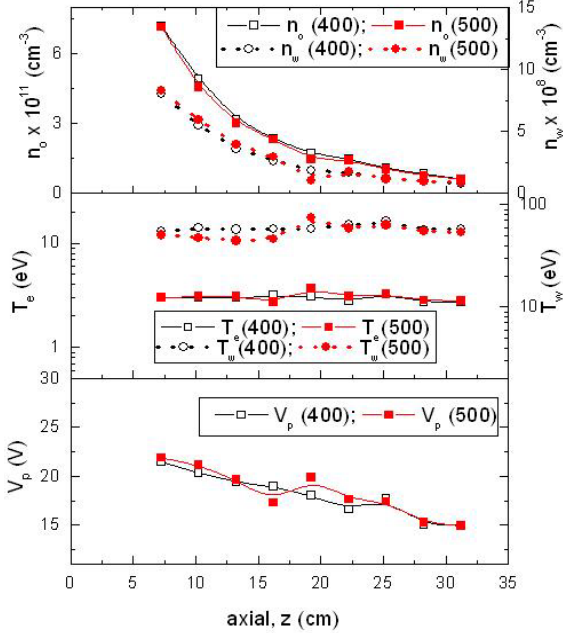


Figure 1 Experimental setup

## 2. Plasma Characterization

Fig. 2(a) presents axial profiles of  $n_0$ ,  $n_w$ ,  $T_e$ ,  $T_w$ , and  $V_p$  for discharges obtained at 400 and 500 W of microwave power (2.45 GHz, cw) at  $\approx 1$  mTorr, argon gas pressure. The data commences from  $z \approx 7.25$  cm (the open end of the CEPS being at  $z \approx 0$ ) to avoid damage to the LP. Fig. 2 shows that there is no

significant difference in the data for power in the range, 400–500 W. Typically,  $n_0 \approx 7.2 \times 10^{11} \text{ cm}^{-3}$  and  $n_w \approx 8.3 \times 10^8 \text{ cm}^{-3}$  at  $z \approx 7.25 \text{ cm}$ , and both densities decrease monotonically with  $z$ . Both  $T_e$  (av.  $\approx 3.0 \text{ eV}$ ) and  $T_w$  (av.  $\approx 50 \text{ eV}$ ) are substantially constant along the axis.



**Figure 2** Axial Profiles of  $n_0$ ,  $n_w$ ,  $T_e$ ,  $T_w$ , and  $V_p$  at argon pressure  $\approx 1 \text{ mTorr}$  and microwave power  $\approx 400$  and  $500$  Watts.

From Fig. 2(c),  $V_p$  is seen to decrease almost linearly from  $\approx 23$  to  $15 \text{ V}$ . Linearity of the plasma potential is a ubiquitous feature of the present experiments. The latter implies a constant electric field, which implies that the plasma in the test chamber is quasineutral.

The data in Fig. 2(a) can be viewed differently by plotting normalized values of the densities with respect to their respective values at  $z \approx 7.25 \text{ cm}$  as in Fig. 3(a). It is seen that the normalized profiles of  $n_0$  and  $n_w$  (shown for  $500 \text{ W}$  only) practically overlap. This feature is found to hold for the other pressures ( $\approx 0.5, 5, 10 \text{ mTorr}$ ) as well [6]. An important feature of the profiles is that the best fits to these are exponentially damped profiles with nearly identical scale length  $\lambda_n \approx 9.0 - 9.5 \text{ cm}$ , even though the pressures differ by more than one order magnitude ( $\approx 0.5 - 10 \text{ mTorr}$ ).

The on-axis magnetic field of the CEPS penetrating the test chamber is shown in Fig. 3(b). The experimental, simulated and best-fit profiles overlap closely, the latter yielding an exponentially damped profile with scale length  $\lambda_M \approx 9.25 \text{ cm}$ .

Since  $T_w \gg V_p$  and  $n_w \ll n_0$  for all pressures and powers, it follows that the warm electrons will be unaffected by the ambipolar electric field or quasineutrality considerations. In light of this and the fact that  $\lambda_n \approx \lambda_M$  we may associate  $\lambda_n$  with  $\lambda_M$ , which implies that both warm and bulk electrons are strongly magnetized, and also explains the pressure independence of  $\lambda_n$ . For the warm electrons,  $r_{Lw} \approx 0.5 \text{ mm}$  near  $z \approx 4.25 \text{ cm}$  and increases to  $\approx 2 \text{ mm}$  near  $z \approx 37 \text{ cm}$ , so that for the most part they may be regarded as strongly magnetized. For the bulk electrons, the situation is even better ( $r_{Le} \approx 0.09 - 0.4 \text{ mm}$ ) on account of their lower temperature.

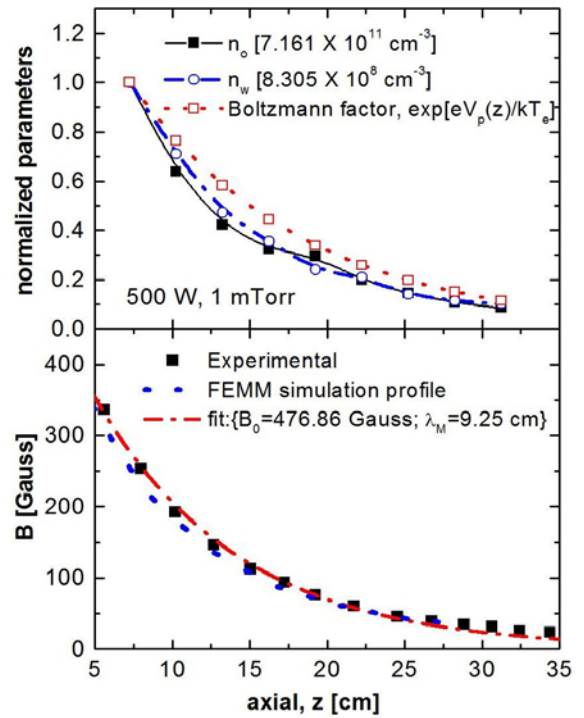


**Figure 3(a)** Axial profiles of normalized  $n_0$  [black solid line and square],  $n_w$  [blue open circle],  $n_{fit}$  [blue dash-dot line] =  $n_0 \exp\{(z-z_0)/\lambda_n\}$ , and the Boltzmann relation  $\exp\{qV_p(z)/kT_e\}$  [red dotted line, open circle] at  $500 \text{ W}$  power and argon pressure  $\approx 1 \text{ mTorr}$ .  $T_e$  is the average temperature. (b) Three profiles of the on-axis magnetic field of the CEPS penetrating the test chamber:  $B_{exptl}$  [black solid square],  $B_{simulated}$  [blue dotted line] and  $B_{fit}(z) = B_0 \exp\{(z-z_M)/\lambda_M\}$  [red dash-dot line],  $z_M = 2.25 \text{ cm}$  and  $\lambda_M \approx 9.25 \text{ cm}$ .

Fig. 3(a) also shows that the *normalized* Boltzmann factor [ $\propto \exp\{V_p(z)/T_e\}$ ] with  $T_e \approx 3 \text{ eV}$  (bulk electron temperature) and  $V_p(z)$  from Fig. 2, overlaps approximately with the normalized  $n_0$  profile, indicating that the bulk electrons are roughly in thermal equilibrium along the system.

Since detailed data are available for different pressures only on the axis, we restrict ourselves to a thin flux tube (of infinitesimal cross-section) centered about field lines near the axis; this also allows us to treat all quantities as functions of  $z$  alone ( $r \approx 0$ ). As already seen from the data, the warm and bulk electron densities, scale as  $\exp\{-z/\lambda_M\}$  along  $z$ . The equation of motion for the bulk electrons reduces to the force balance condition between the electric and pressure terms [7]:  $E = -\{T_e/en_0\}[dn_0/dz]$ , where  $E$  is the ambipolar electric field along  $z$ ,  $e$ , the electron charge, and  $T_e$ , the electron temperature in energy units. The latter simply yields the Boltzmann relation for the bulk electrons (Figs. 3). (Thermal equilibrium will hold for the bulk electrons also along field lines not on the axis.) The requirement that  $n_0(z)$  vary exponentially with  $z$ , forces  $E$  to be a constant ( $\approx T_e/\lambda_M e$ ) as found in the experiments (Fig. 2(c)).

The rates of creation of electron-ion pairs per unit volume of the tube, by impact ionization of gas atoms by bulk and warm electrons are given by,  $B = \nu_{ib}n_0$  and  $W = \nu_{iw}n_w$  respectively, where  $\nu_{ib}$  ( $\nu_{iw}$ ) is the ionization frequency for bulk (warm) electrons on neutral gas atoms (including charge exchange). Likewise, the rate of flow of plasma *into* unit volume of the tube from the CEPS is given by,  $A = -d\Gamma_i/dz$ , where  $\Gamma_i$  is the axial ion flux and may be determined from the steady-state ion equation of motion [7]. The total rate at which particles are added within unit volume of the tube is given by,  $R = A + B + W$ ; in steady state  $R$  equals the radial *loss* rate of plasma from the tube.

Table I: Comparison of different plasma production mechanisms in non-ECR zones

| $P$<br>(mTorr) | $P \approx 400$ W<br>(500 W) |                  |                  |
|----------------|------------------------------|------------------|------------------|
|                | $A/R$                        | $B/R$            | $W/R$            |
| 0.5            | 0.866<br>(0.834)             | 0.054<br>(0.083) | 0.080<br>(0.083) |
| 1.0            | 0.585<br>(0.595)             | 0.237<br>(0.225) | 0.179<br>(0.180) |
| 5.0            | 0.252<br>(0.196)             | 0.185<br>(0.293) | 0.564<br>(0.510) |
| 10.0           | 0.134<br>(0.131)             | 0.149<br>(0.130) | 0.717<br>(0.739) |

Using  $n/n_w$  values [ $\sim 925$  (at 0.5 mTorr) – 1200 (at 10 mTorr)] and other data from the experiments, one may compute the normalized (dimensionless) rates,  $A/R$ ,  $B/R$  and  $W/R$ . These are summarized in Table I for different pressures  $p$  and two microwave power levels  $P$ .

Ionization by bulk electrons ( $= B/R$ ) shows a broad maximum at intermediate pressures, but remains essentially small ( $< 25\%$ ). Plasma flow from the CEPS ( $= A/R$ ) is the primary plasma filling mechanism at low pressures, while ionization by warm electrons ( $= W/R$ ) is the dominant mechanism with increasing pressure. Most importantly, there exists a regime of operation of ECR discharges at high pressures, where high-density plasma in non-resonance regions is maintained chiefly by a low-density population of warm electrons arriving from the CEPS.

### 3. Conclusions

Characterization of the CEPS plasma using a test chamber has provided insight as to how the plasma formation in the non-resonance regions changes with the pressure. The knowledge should be useful for designing systems with large non-resonance volumes (at high and low pressures) as well as low-pressure applications as in plasma thrusters.

### 4. References

- [1] A. Ganguli, et al, *Proceedings of PPPS-2013 held in San Francisco, California, USA*, Publ. IEEE & POD Publ. Curran Associates, Inc. ISBN: 978-1-4673-5166-9, **1**, (2014) 327
- [2] R. D. Tarey, et al, *Proceedings of PPPS-2013 held in San Francisco, California, USA*, Publ. IEEE & POD Publ. Curran Associates, Inc. ISBN: 978-1-4673-5166-9, **1**, (2014) 332
- [3] N. Arora, *Ph.D. Thesis*, IIT Delhi, New Delhi, (2014)
- [4] B. B. Sahu, A. Ganguli, R. D. Tarey, *Plasma Sources Sci. Technol.* **23** (2014) 065050
- [5] B. B. Sahu, R. D. Tarey, A. Ganguli, *Phys. Plasmas* **21** (2014) 023504
- [6] To be communicated
- [7] M. A. Lieberman and A. J. Lichtenberg, *Principles of Plasma Discharges and Materials Processing*, (John Wiley & Sons, Hoboken, NJ, 2005).